JPhys Materials

PAPER • OPEN ACCESS

Biaxial strain tuning of interlayer excitons in bilayer MoS_2

To cite this article: Felix Carrascoso *et al* 2020 *J. Phys. Mater.* **3** 015003

JPhys Materials

PAPER

Biaxial strain tuning of interlayer excitons in bilayer MoS_2

Felix Carrascoso[1], **Der-Yuh Lin**[2], **Riccardo Frisenda**[1,3] **and Andres Castellanos-Gomez**[1,3]

[1] Materials Science Factory, Instituto de Ciencia de Materiales de Madrid (ICMM), Consejo Superior de Investigaciones Científicas (CSIC), Sor Juana Inés de la Cruz 3, E-28049 Madrid, Spain
[2] National Changhua University of Education, Bao-Shan Campus, No. 2, Shi-Da Rd, Changhua City 500, Taiwan, ROC
[3] Authors to whom any correspondence should be addressed.

E-mail: riccardo.frisenda@csic.es **and** andres.castellanos@csic.es

Keywords: 2D materials, molybdenum disulfide (MoS_2), interlayer exciton, strain engineering, bilayer

Supplementary material for this article is available online

OPEN ACCESS

RECEIVED
9 August 2019

REVISED
6 September 2019

ACCEPTED FOR PUBLICATION
13 September 2019

PUBLISHED
30 October 2019

Abstract

We show how the excitonic features of biaxial MoS_2 flakes are very sensitive to biaxial strain. We find a lower bound for the gauge factors of the A exciton and B exciton of (-41 ± 2) meV/% and (-45 ± 2) meV/% respectively, which are larger than those found for single-layer MoS_2. Interestingly, the interlayer exciton feature also shifts upon biaxial strain but with a gauge factor that is systematically larger than that found for the A exciton, (-48 ± 4) meV/%. We attribute this larger gauge factor for the interlayer exciton to the strain tunable van der Waals interaction due to the Poisson effect (the interlayer distance changes upon biaxial strain).

The isolation of atomically thin MoS_2 by mechanical exfoliation in 2010 opened the door to study the intriguing optical properties of this 2D semiconductor material [1–3]. In fact, MoS_2 and other members of the transition metal dichalcogenide family show a rich plethora of exitonic physical phenomena, present even at room temperature. Mak *et al* and Splendiani *et al* observed a strong thickness dependent photoluminescence emission and a direct-to-indirect band gap transition [1, 2]. MoS_2 also has tightly bound negative trions, an exciton quasiparticle composed of two electrons and a hole [4, 5], and several groups in parallel reported the valley polarization, the selective population of one valley, by pumping with circularly polarized light [6–8]. Moreover, heterostructures built with these 2D systems have also attracted the interest of the scientific community because of the presence of interlayer excitons: excitons formed by electrons and holes that live in different layers [9–13]. Very recently, Gerber *et al* and Slobodeniuk *et al* demonstrated that naturally stacked bilayer MoS_2 (2H-polytype) also presents interlayer excitons, with high binding energy, that can be observed at room temperature [14, 15] and Niehues *et al* demonstrated that uniaxial strain could be used to tune the energy of the interlayer exciton [16].

In this work we employ biaxial strain to modify the band structure, and thus the excitonic resonances, in bilayer MoS_2 flakes. We observe that both the A and B excitons, as well as the interlayer exciton, substantially redshift upon biaxial tension. Interestingly, unlike to what has been reported for uniaxial strain, we found that the interlayer exciton is more effectively tuned upon straining than the A and B excitons. We attribute this effect to a modification of the interlayer interaction as an in-plane biaxial expansion of the bilayer MoS_2 is expected to come hand-by-hand of an out-of-plane compression due to the MoS_2 Poisson's ratio.

MoS_2 flakes were prepared by mechanical exfoliation of bulk natural molybdenite (Moly Hill mine, QC, Canada) with Nitto tape (SPV 224). The cleaved MoS_2 flakes are then transferred to a Gel-Film (WF 4 × 6.0 mil Gel-Film from Gel-Pak®, Hayward, CA, USA). The flakes are optically identified, and their number of layers are determined from quantitative analysis of transmission mode optical microscopy images and micro- transmittance/reflectance spectroscopy [17–19]. Once a suitable bilayer MoS_2 flake is located it is transferred onto a polypropylene (PP) substrate by an all-dry deterministic transfer method [20, 21].

Figure 1(a) shows a reflection mode optical microscopy image of a MoS_2 flake transferred onto PP. Figure 1(b) shows differential reflectance spectra acquired on a mono-, bi- and tri-layer MoS_2 flake with a home-built micro-reflectance microscope. We direct the reader to [22] for technical details about the experimental

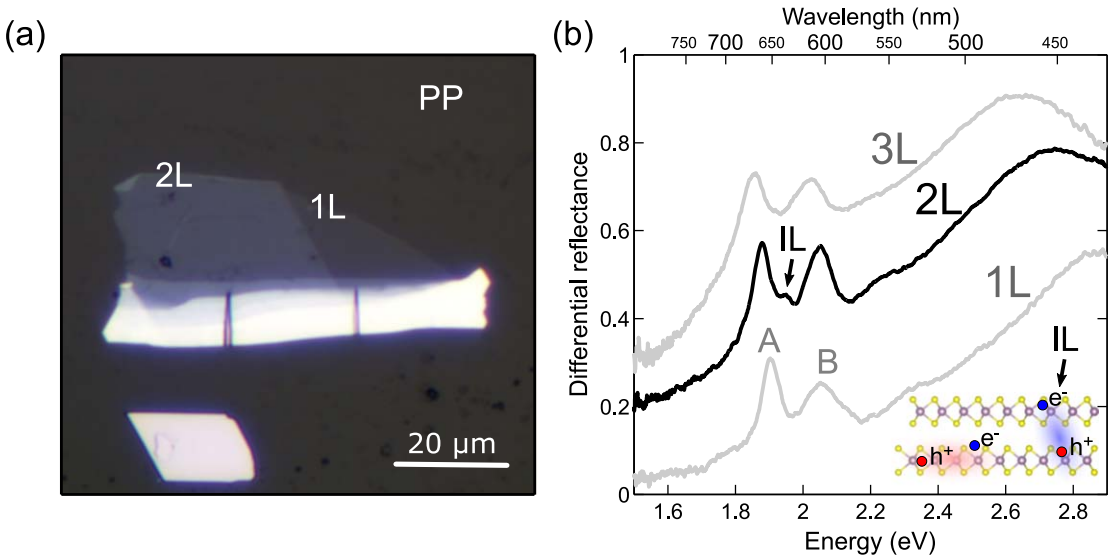

Figure 1. (a) Reflection mode optical microscopy image of a MoS_2 flake with single- and bi-layer regions (highlighted with 1L and 2L respectively) transferred onto the surface of a polypropylene (PP) substrate. (b) Differential reflectance spectra acquired on single-, bi- and tri-layer MoS_2 flakes on PP. The A and B excitons are clearly visible for all these thicknesses while the interlayer (IL) exciton, present in multilayer MoS_2, is more clearly visible for the bilayer flake.

setup. To obtain the differential reflectance spectra we first collect the light reflected from the substrate (R_s) by means of a fiber-coupled compact CCD spectrometer (see Materials and methods section). Then we collect the light reflected by the desired MoS_2 flake (R_f) and we calculate the differential reflectance as: $\Delta R/R = 1 - R_s/R_f$ [19, 23]. All the spectra displayed in figure 1(b) show two strong transitions in all of them assigned to the A and B excitons (~1.9 eV and ~2.05 eV respectively) originated from direct band gap transitions at the K point of the Brillouin zone [1, 2]. Interestingly, in bilayer MoS_2 one can see another prominent peak between the A and B excitons. That peak can be also observed in trilayer and even multilayer MoS_2 but it cannot be as easily resolved as in the case of bilayer MoS_2. This feature in the reflectance spectra have been recently demonstrated (through temperature dependent optical spectroscopy studies, magneto-optical measurements and density functional theory calculations) to be originated by the generation of interlayer (IL) excitons [14, 15, 24]. These excitons are, similarly to the A and B excitons, due to direct transitions at the K point but unlike them the electron and hole are spatially separated in the different MoS_2 layers (see the cartoon in figure 1(b)).

Uniaxial and biaxial strain have been proven to be effective methods to modify the optical properties of 2D semiconductors [25–28]. Here, in order to biaxially strain the MoS_2 bilayers we exploit the large thermal expansion mismatch between the PP substrate (~130×10^{-6} K^{-1}) and MoS_2 (1.9×10^{-6} K^{-1}) [29]. PP has also a relatively high Young's modulus (1.5–2 GPa) for a polymer, which is essential to guarantee an optimal strain transfer from substrate to flake. One can then biaxially stretch (or compress) the flakes by warming up (or cooling down) the substrate [30–32]. We used a Peltier element to control the temperature of the substrate around room temperature (27 °C–28 °C) that allows us to cool down to 17 °C (−0.13%) and to warm up to 95 °C (+0.87%). The substrate temperature can be translated to biaxial expansion/compression through the thermal expansion coefficient of PP (see the supporting information available online at stacks.iop.org/JPMATER/3/015003/mmedia).

Figure 2(a) shows the differential reflectance spectra acquired at different substrate temperatures from 19 °C to 91 °C. The spectra redshift upon temperature increase above room temperature and blueshift when the substrate is cooled down below room temperature. The spectra can be fitted to a sum of three Gaussian peaks in order to extract the energy position of the A, B and IL excitons. The summary of the exciton energy positions is shown in figure 2(b). From this figure one can extract the spectral shift per °C for the different excitons: (-0.93 ± 0.03) meV $°C^{-1}$ for the A exciton and (-0.97 ± 0.03) meV $°C^{-1}$ for the B exciton. In order to disentangle the intrinsic spectral shift expected for MoS_2 upon temperature change from that originated from the biaxial strain we fabricated a MoS_2 sample on a Si substrate with 50 nm of SiO_2, which is expected to have a negligible thermal expansion, and we probe the exciton position as a function of temperature. We found that for single-, bi- and tri-layer MoS_2 all the excitons shift by −0.4 meV $°C^{-1}$. By subtracting this intrinsic thermal shift value to the values measured in samples fabricated on PP we can determine the spectral shift induced by biaxial strain. And we can determine the gauge factor, the spectral shift per % of biaxial strain, by calculating the substrate biaxial expansion (or compression) upon temperature change (see the supporting information for

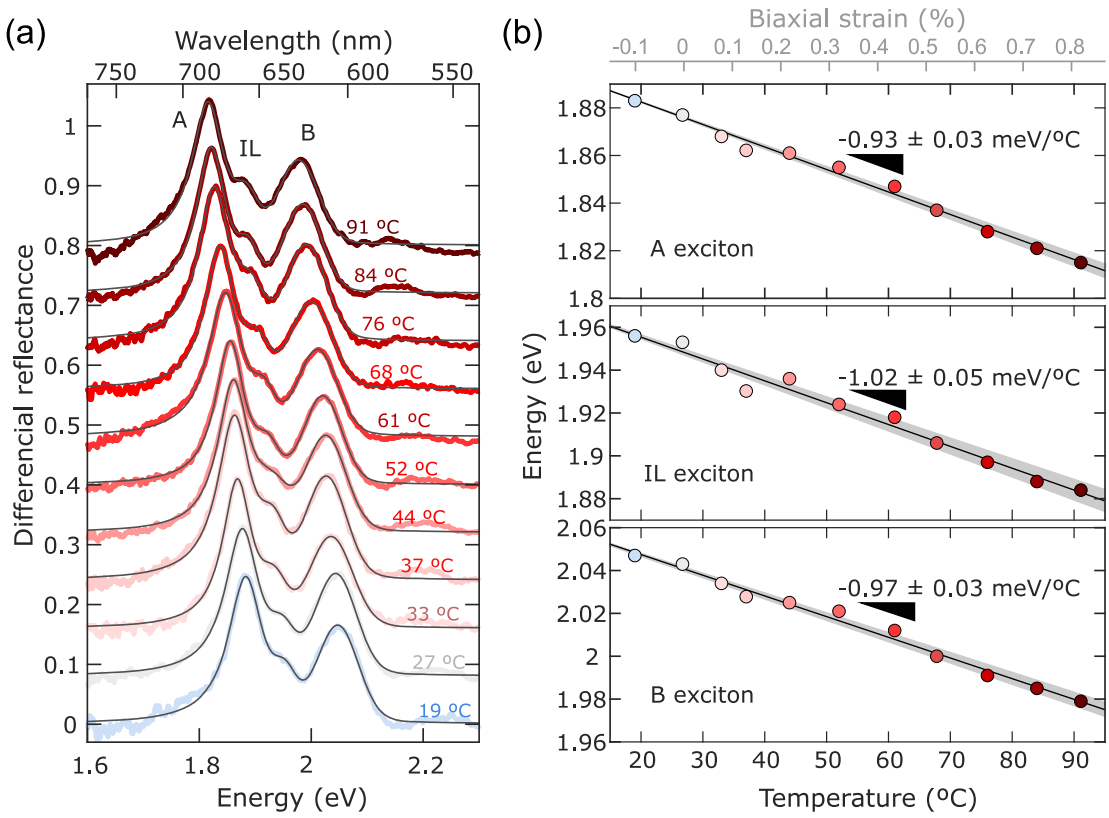

Figure 2. (a) Differential reflectance spectra of a MoS_2 bilayer deposited on PP recorded at different temperatures (quadratic polynomial background removed). The black solid lines represent the total fit to the data (composed of three Gaussian peaks). (b) energy of the A, B and IL excitonic peaks extracted from the fit and plotted as a function of the substrate temperature (bottom axis) and of the substrate biaxial strain (top axis). Note that the uncertainty of the exciton energies determined through the fits is below 0.1% of their value.

details about the thermal expansion calibration of the PP substrates). The resulting gauge factors for the A and B excitons are (-41 ± 2) meV/% and (-45 ± 2) meV/%. Note that these gauge factor values should be considered as a lower bound as we are assuming that all the biaxial expansion of the substrate can be effectively translated to biaxial strain to the MoS_2 flake. Due to the Young's modulus mismatch between the PP substrate and the MoS_2 the strain transfer efficiency could be lower (and thus we would be underestimating the gauge factor values) [30, 33]. The fact that all the spectra shows a clear IL peak indicates that both MoS_2 layers are equally strained (maintaining the 2H- stacking during the whole straining cycle) as the presence of IL exciton peaks is extremely sensitive to the relative atomic arrangement between the layers [14]. We also direct the reader to the supporting information section S6 for a finite element simulation used to estimate the strain transfer along the thickness of thick multilayered MoS_2 flakes.

It is interesting to note that all the bilayer MoS_2 flakes studied here have A and B exciton gauge factors that are substantially larger than those found for single-layer flakes which are in the –(10–25) meV/% range [30], in agreement with density functional theory calculations [34]. We point the reader to the supporting information for a summary of the measured datasets in 2 single-layer flakes, other 5 bilayers and one trilayer flake.

For the interlayer exciton we find a gauge factor of (-48 ± 4) meV/% which is substantially larger than that found for the A exciton. We direct the reader to the supporting information for datasets acquired on other five bilayer MoS_2 flakes (with gauge factor up to -55 meV/%) and one trilayer flake that also have a substantially larger gauge factor for the interlayer exciton (-23 meV/%) than for the A exciton (-11 meV/%) similarly to the bilayer case. This contrasts with what has been recently reported for uniaxially strained bilayer MoS_2 flakes by Niehues *et al* where the gauge factor of the interlayer exciton was slightly lower than that of the A exciton. We attribute the larger gauge factor observed in our experiment to a reduction (or increase) of the bilayer interlayer spacing upon biaxial tension (or compression) as expected from the Poisson effect: as the out-of-plane Poisson's ratio of MoS_2 is $\nu_o \sim 0.2$ a biaxial tension of 1% would yield a reduction of 0.2% in the interlayer distance [35]. A similar tunability of the interlayer van der Waals interaction upon biaxial strain has been recently reported in black phosphorus by Huang and co-workers [36]. The strain tunable interlayer distance could explain the large gauge factor observed for bilayer MoS_2 upon biaxial strain as Deilmann and Thygesen demonstrated through density functional theory calculations that the interlayer exciton position strongly depends on the interlayer

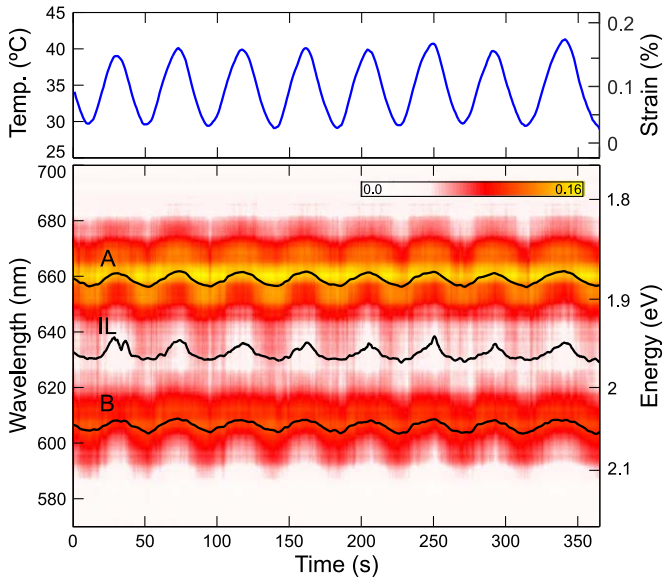

Figure 3. Time evolution of the differential reflectance spectra of bilayer MoS_2 (bottom axis) while the temperature of the substrate is cycled between 30 °C and 40 °C (top axis). The intensity of the differential reflectance spectra is displayed in the color axis of the colormap. The A, B and IL exciton position is also displayed through the black solid lines.

distance [24]. In previous uniaxial strain works, on the other hand, because of the Poisson's ratio of the polycarbonate substrate ($\nu = 0.37$) when the flake is uniaxially stretched in one direction it is compressed in the perpendicular direction (within the basal plane) [37] counteracting most of the Poisson's effect induced upon uniaxial tension [16].

In figure 3 we test the reproducibility of the biaxial strain tuning exploiting the thermal expansion of the substrate. We modulated the temperature of the substrate between ~30 °C and ~40 °C (see the registered temperature versus time in the top panel of figure 3). The color map in the bottom panel shows the time evolution of the differential reflectance spectra and the extracted position of the A, IL and B excitons, extracted from fits similarly to figure 2(a), are displayed with the black lines. This illustrates the power of this method to tune the van der Waals interlayer interaction and thus the interlayer excitons in biaxial MoS_2.

Conclusions

In summary, we have exploited the large thermal expansion of polypropylene substrates to subject biaxial MoS_2 flakes to biaxial strain. We find that the excitons redshift upon biaxial tension with gauge factors that are larger than those reported for monolayer MoS_2. Interestingly, the interlayer exciton gauge factor is systematically larger than that of the A and B excitons (contrasting the results reported for uniaxially strained bilayer MoS_2). We attribute this larger gauge factor of the interlayer exciton to the strain tuning of the van der Waals interaction upon biaxial in-plane straining due to the Poisson effect.

Materials and methods

Optical microscopy images have been acquired with a Motic BA MET310-T upright metallurgical microscope equipped with an AM Scope MU1803 camera with 18 megapixels. The trinocular of the microscope has been modified to connect it to a fiber-coupled Thorlabs spectrometer (part number: CCS200/M) to perform the differential reflection spectroscopy measurements [19].

Acknowledgments

This project has received funding from the European Research Council (ERC) under the European Union's Horizon 2020 research and innovation programme (grant agreement n° 755655, ERC-StG 2017 project 2D-TOPSENSE). ACG acknowledge funding from the EU Graphene Flagship funding (Grant Graphene Core 2, 785219). RF acknowledges support from the Spanish Ministry of Economy, Industry and Competitiveness through a Juan de la Cierva-formación fellowship 2017 FJCI-2017-32919. D-Y L acknowledges financial support

from the Ministry of Science and Technology of Taiwan, Republic of China under contract No. MOST 108-2221-E-018-010.

ORCID iDs

Riccardo Frisenda https://orcid.org/0000-0003-1728-7354
Andres Castellanos-Gomez https://orcid.org/0000-0002-3384-3405

References

[1] Mak K F, Lee C, Hone J, Shan J and Heinz T F 2010 Atomically thin MoS_2: a new direct-gap semiconductor *Phys. Rev. Lett.* **105** 136805
[2] Splendiani A *et al* 2010 Emerging photoluminescence in monolayer MoS_2 *Nano Lett.* **10** 1271–5
[3] Castellanos-Gomez A, Agrat N and Rubio-Bollinger G 2010 Optical identification of atomically thin dichalcogenide crystals *Appl. Phys. Lett.* **96** 213116
[4] Mak K F *et al* 2013 Tightly bound trions in monolayer MoS_2 *Nat. Mater.* **12** 207–11
[5] Ross J S *et al* 2013 Electrical control of neutral and charged excitons in a monolayer semiconductor *Nat. Commun.* **4** 1474
[6] Mak K F, He K, Shan J and Heinz T F 2012 Control of valley polarization in monolayer MoS_2 by optical helicity *Nat. Nanotechnol.* **7** 494–8
[7] Zeng H, Dai J, Yao W, Xiao D and Cui X 2012 Valley polarization in MoS_2 monolayers by optical pumping *Nat. Nanotechnol.* **7** 490–3
[8] Cao T *et al* 2012 Valley-selective circular dichroism of monolayer molybdenum disulphide *Nat. Commun.* **3** 887
[9] Ross J S *et al* 2017 Interlayer exciton optoelectronics in a 2D heterostructure p–n junction *Nano Lett.* **17** 638–43
[10] Rivera P *et al* 2015 Observation of long-lived interlayer excitons in monolayer $MoSe_2$–WSe_2 heterostructures *Nat. Commun.* **6** 6242
[11] Yu Y *et al* 2014 Equally efficient interlayer exciton relaxation and improved absorption in epitaxial and nonepitaxial MoS_2/WS_2 heterostructures *Nano Lett.* **15** 486–91
[12] Baranowski M *et al* 2017 Probing the interlayer exciton physics in a MoS_2/$MoSe_2$/MoS_2 van der Waals heterostructure *Nano Lett.* **17** 6360–5
[13] Nagler P *et al* 2017 Interlayer exciton dynamics in a dichalcogenide monolayer heterostructure *2D Mater.* **4** 25112
[14] Gerber I C *et al* 2019 Interlayer excitons in bilayer MoS_2 with strong oscillator strength up to room temperature *Phys. Rev.* B **99** 35443
[15] Slobodeniuk A O *et al* 2019 Fine structure of K-excitons in multilayers of transition metal dichalcogenides *2D Mater.* **6** 25026
[16] Niehues I, Blob A, Stiehm T and de Vasconcellos S M 2019 Interlayer excitons in bilayer MoS_2 under uniaxial tensile strain *Nanoscale* **11** 12788–12792
[17] Niu Y *et al* 2018 Thickness-dependent differential reflectance spectra of monolayer and few-layer MoS_2, $MoSe_2$, WS_2 and WSe_2 *Nanomaterials* **8** 725
[18] Taghavi N S *et al* 2019 Thickness determination of MoS_2, $MoSe_2$, WS_2 and WSe_2 on transparent stamps used for deterministic transfer of 2D materials *Nano Res.* **12** 1–5
[19] Frisenda R *et al* 2017 Micro-reflectance and transmittance spectroscopy: a versatile and powerful tool to characterize 2D materials *J. Phys. D: Appl. Phys.* **50** 074002
[20] Castellanos-Gomez A *et al* 2014 Deterministic transfer of two-dimensional materials by all-dry viscoelastic stamping *2D Mater.* **1** 011002
[21] Frisenda R *et al* 2018 Recent progress in the assembly of nanodevices and van der Waals heterostructures by deterministic placement of 2D materials *Chem. Soc. Rev.* **47** 53–68
[22] Frisenda R *et al* 2017 Micro-reflectance and transmittance spectroscopy: a versatile and powerful tool to characterize 2D materials *J. Phys. D: Appl. Phys.* **50** 074002
[23] Dhakal K P *et al* 2014 Confocal absorption spectral imaging of MoS_2: optical transitions depending on the atomic thickness of intrinsic and chemically doped MoS_2 *Nanoscale* **6** 13028–35
[24] Deilmann T and Thygesen K S 2018 Interlayer excitons with large optical amplitudes in layered van der Waals materials *Nano Lett.* **18** 2984–9
[25] Conley H J *et al* 2013 Bandgap engineering of strained monolayer and bilayer MoS_2 *Nano Lett.* **13** 3626–30
[26] He K, Poole C, Mak K F and Shan J 2013 Experimental demonstration of continuous electronic structure tuning via strain in atomically thin MoS_2 *Nano Lett.* **13** 2931–6
[27] Hui Y Y *et al* 2013 Exceptional tunability of band energy in a compressively strained trilayer MoS_2 sheet *ACS Nano* **7** 7126–31
[28] Schmidt R *et al* 2016 Reversible uniaxial strain tuning in atomically thin WSe_2 *2D Mater.* **3** 021011
[29] El-Mahalawy S H and Evans B L 1976 The thermal expansion of 2H-MoS_2, 2H-$MoSe_2$ and 2H-WSe_2 between 20 and 800 C *J. Appl. Crystallogr.* **9** 403–6
[30] Frisenda R *et al* 2017 Biaxial strain tuning of the optical properties of single-layer transition metal dichalcogenides *Npj 2D Mater. Appl.* **1** 10
[31] Frisenda R *et al* 2017 Biaxial strain in atomically thin transition metal dichalcogenides *Proc. SPIE—The Int. Society for Optical Engineering* **10353** 103530N
[32] Plechinger G *et al* 2015 Control of biaxial strain in single-layer molybdenite using local thermal expansion of the substrate *2D Mater.* **2** 015006
[33] Liu Z *et al* 2014 Strain and structure heterogeneity in MoS_2 atomic layers grown by chemical vapour deposition *Nat. Commun.* **5** 5246
[34] Scalise E, Houssa M, Pourtois G, Afanas'ev V and Stesmans A 2011 Strain-induced semiconductor to metal transition in the two-dimensional honeycomb structure of MoS_2 *Nano Res.* **5** 43–8
[35] Woo S, Park H C and Son Y-W 2016 Poisson's ratio in layered two-dimensional crystals *Phys. Rev.* B **93** 75420
[36] Huang S *et al* 2019 Strain-tunable van der Waals interactions in few-layer black phosphorus *Nat. Commun.* **10** 2447
[37] Island J O *et al* 2016 Precise and reversible band gap tuning in single-layer $MoSe_2$ by uniaxial strain *Nanoscale* **8** 2589–2593